Morphological, Transport, and Adsorption Properties of Ethylene Vinyl Acetate/Polyurethane/Bentonite Clay Composites

Derrick S. Dlamini, Ajay K. Mishra, Bhekie B. Mamba

Department of Chemical Technology, University of Johannesburg, P. O. Box 17011, Doornfontein 2028, Johannesburg, South Africa

Received 17 June 2011; accepted 7 September 2011
DOI 10.1002/app.35600
Published online 11 December 2011 in Wiley Online Library (wileyonlinelibrary.com).

ABSTRACT: The effect of polyurethane (PU) foam on the morphological and transport properties of ethylene vinyl acetate (EVA) with 9% vinyl acetate and the potential application of 3%bentonite/28.5% PU/68.5% EVA composites fabricated via the melt-blending method in heavy-metal extraction from water systems were investigated. EVA did not swell in water, whereas the PU/EVA blend attained a maximum percentage of deionized water uptake of 2.158 mol %. A 3% bentonite/28.5% PU/68.5% EVA composite blend successfully removed 90% of Pb^{2+} from an aqueous solution with an initial concentration of 30 mg/L, whereas 3% bentonite/97% EVA could only extract 7.323% of Pb^{2+} ions. Pb^{2+} adsorption was found to obey the Langmuir adsorption isotherm and pseudo-second-order kinetic model. Thermodynamic studies demonstrated that the adsorption was favorable at room temperature and the uptake of Pb^{2+} was mostly by physical adsorption, as also indicated by the value $n = 2.449$ (where n is an empirical parameter indicating transport mode) from the Freundlich adsorption isotherm. © 2011 Wiley Periodicals, Inc. J Appl Polym Sci 124: 4978–4985, 2012

Key words: adsorption; crystallization; microstructure; phase behavior; synthesis

INTRODUCTION

The pollution of water resources due to the disposal of heavy metals and organic substances, especially from industrial activities, has been causing worldwide concern over the past few decades. Some heavy metals are capable of being assimilated, stored, and concentrated in the human body and may cause nausea, salivation, muscular cramps, renal degradation, and skeletal deformity.[1] The most problematic metals include arsenic (As), lead (Pb), and mercury (Hg), to mention a few. Unlike organic water pollutants, heavy metals are not susceptible to biodegradation and photodegradation.[2]

The removal of heavy-metal ions from sewage effluents and other water resources is essential to ensuring environmental and human safety. Several techniques, such as reverse osmosis, filtration, ion exchange, and adsorption are applied to remove water pollutants. Adsorption is considered a simple and economically viable method for water pollutant removal.[3] Activated carbon is the most widely applied adsorbent because it has a high degree of microporosity, with a concomitant high surface area, ideal micropore volume, large adsorption capacity, and fast adsorption kinetics.[4] Activated carbon is used in a powder form; therefore, there is a problem with handling and incomplete recovery.

In the past decade, more research has been focused on embedding powder adsorbates into the polymer matrix to ensure better recovery. The results have been very promising. For instance, polymer/clay composites were found to have potential application in adsorption technology for water treatment.[5] Unfortunately, the research focused on hydrophilic polymers, and the composites were fabricated via the solution-blending technique. Hydrophilic polymers can easily lose stability in water environments, and there is the risk of environmental pollution because the solution remaining from the blending may leach into the water. Therefore, to enhance the stability, it is ideal to use hydrophobic polymers, perhaps blended with hydrophilic polymers to ensure that there is adequate water absorption. The risk of environmental pollution can be eliminated with the melt-blending technique, which further necessitates the need to incorporate a hydrophobic polymer because mostly thermoplastics are used for this technique.

In this study, polyurethane (PU) foam was used to improve the water penetration in an ethylene vinyl acetate (EVA)/bentonite composite fabricated via the

Correspondence to: A. K. Mishra (amishra@uj.ac.za).
Contract grant sponsors: National Research Foundation, University of Johannesburg.

melt-blending technique. EVA with 9% vinyl acetate (VA) is hydrophobic and, therefore, stable in a water environment. In addition, EVA with bentonite clay is compatible with the melt-blending method of composite fabrication. On the other hand, PU with bentonite clay has a high affinity for water, and it is not compatible with the melt-blending method. It was expected that the blending of these two polymers would produce a blend that could be suitable for better adsorption and transport properties. To the best of our knowledge, the adsorption and transport properties of such polymer blends have not been previously reported. The EVA/PU blend and the polymer/clay composite were characterized for morphological properties by means of scanning electron microscopy (SEM). Immersion tests were undertaken to investigate the transport properties in the EVA/PU blend. The bentonite/EVA/PU composite was used for the removal of Pb^{2+} from water.

EXPERIMENTAL

Materials

Bentonite Ocean MD with 95% montmorillonite was supplied by G&W Minerals (Wadeville, South Africa). PU foam was supplied by SASOL Polymers (South Africa). EVA with a 9% VA content was obtained from Plastamid (Johannesburg, South Africa). $AgNO_3$, $Ni(NO_3)_2{\cdot}6H_2O$, $Pb(NO_3)_2$, and $FeCl_3{\cdot}6H_2O$ were purchased from Merck Chemicals (Johannesburg, South Africa), and concentrated HCl and KOH were procured from Aldrich Chemicals (Johannesburg, South Africa).

Fabrication of the composites

To prepare the blend, EVA and PU were mixed in a Rheomix. The EVA/PU ratios were 90 : 10, 80 : 20, 70 : 30, 60 : 40, and 50 : 50% (w/w). The Thermo Scientific Haake Rheomix OS was equipped with roller-type rotors at 100°C and a rotational speed of 60 rpm/min for a 30-min residence time. The mixing chamber occupied was 64 cm^3. The blend was chopped into small chips, which were then molded into rectangular sheets with dimensions of 500 × 50 × 1 mm^3 by extrusion with a single-screw extruder. After characterization (water sorption), a ratio of 68.5 : 28.5 was selected for the fabrication of the bentonite/PU/EVA composite with a 3% (w/w) bentonite loading with the same procedure.

Characterization

SEM

The surface morphology was examined with a JEOL5600 SEM instrument. Specimens were deposited on double-sided carbon conductive scotch tape and examined on the surface after double coating with carbon for charge accumulation.

Swelling tests

The samples were cut into rectangular sheets with dimensions of 100 × 40 × 1 mm^3. The experiments were done in plastic-capped brown bottles with deionized water. At specified intervals of time, the specimens were removed from the bottles; penetrants adhering onto the surfaces were removed by gentle pressing of the samples between soft filter papers with minimum pressure and then the weighing of the samples immediately with an analytical balance. The weighing of the samples continued until the specimens attained equilibrium. The percentage water uptake at time t [Q_t (mol %)] of the immersed composite specimen was calculated with the following equation:[6]

$$Q_t = \frac{\text{Mass of water sorbed/Molar mass of water}}{\text{Mass of the composite}} \times 100\% \quad (1)$$

Batch adsorption studies

A stock Pb^{2+} solution (200 mg/L) was prepared by the dissolution of 0.319 g of $Pb(NO_3)_2$ salt in deionized water. Batch adsorption experiments were conducted to establish the optimum pH, contact time, initial concentration, and effect of the temperature on the uptake of Pb^{2+}. The adsorbent weight was 20 mg, and the volumes of the analyte solutions were about 20 mL. The initial pH of the solution was adjusted with 0.1*M* KOH or HCl. The effect of the competitive adsorption of Pb^{2+} was investigated in the presence of Ag^+, Ni^{2+}, and Fe^{3+} as interfering ions in binary-component systems at equal concentrations (100 mg/L). After adsorption, the solutions were analyzed for any remaining Pb^{2+} concentration with atomic adsorption spectroscopy.

RESULTS AND DISCUSSION

Surface morphology

Figure 1 shows typical SEM images of the neat EVA and 10% PU/90% EVA, 30% PU/70% EVA, and 3%bentonite/28.5% PU/68.5% EVA composites. The SEM image of EVA [Fig. 1(A)] depicts a woven surface morphology.

As can be seen in Figure 1(B), after 10% PU was added, the woven morphology of EVA disappeared, and at a 30% PU loading, the blend attained a porous surface morphology, as depicted in Figure 1(C). The pores shown in Figure 1(C) appeared to be less regular

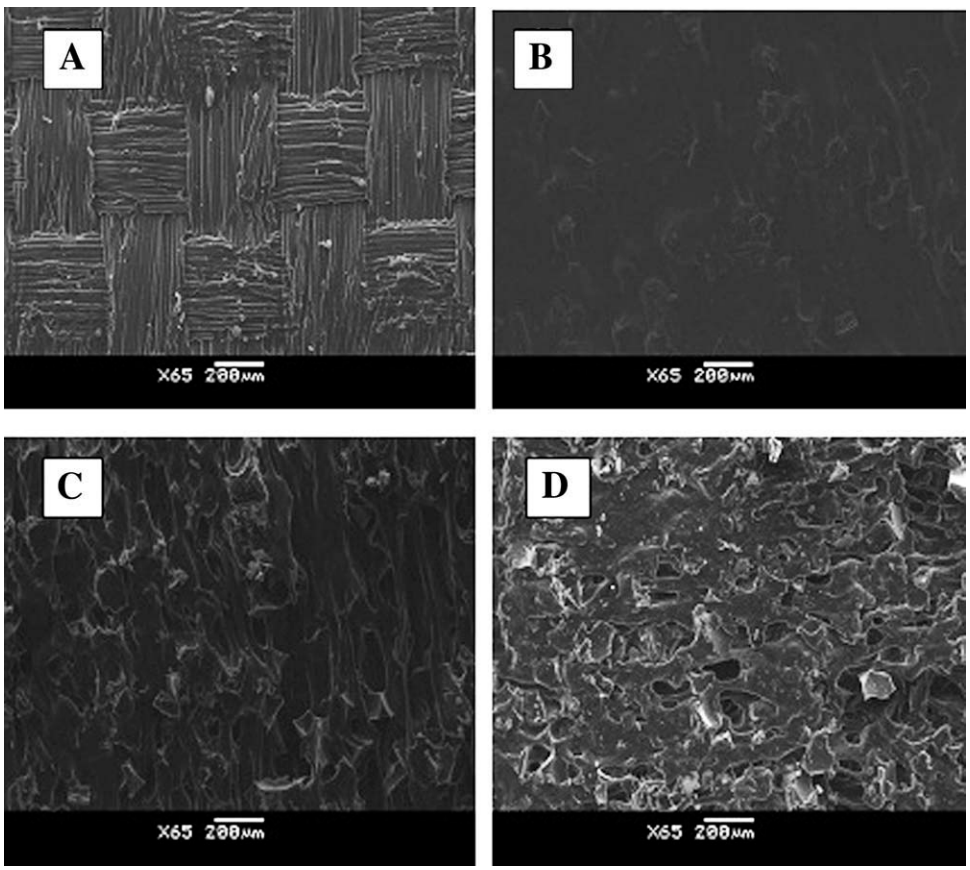

Figure 1 SEM images of (A) EVA and the (B) 10% PU/90% EVA, (C) 30% PU/70% EVA, and (D) 3%bentonite/28.5% PU/68.5% EVA composites.

compared to the composite pores shown in Figure 1(D). The pores may have resulted from the expansion and opening of PU during thermal blending.

Membrane studies

Water sorption

The experimental results for the immersion of the PU/EVA blend and EVA are shown in Figure 2.

The percentage water uptake time profile for EVA highlighted the hydrophobic nature of the polymer. The blending of EVA with PU improved the water sorption behavior of EVA. This observation was attributed to the porous surface morphology of the blend, as shown by SEM.

Transport mechanism

To investigate the transport mechanism of water molecules through the polymer blend, the following equation was applied:[7]

$$\log \frac{Q_t}{Q_\infty} = \log k + n \log t \qquad (2)$$

where Q_∞ is the equilibrium water uptake (mol %) and k and n are empirical parameters. The value of n indicates the transport mode; for instance, a value of $n = 0.5$ suggests the Fickian diffusion mode, and for $n = 1$, a non-Fickian diffusion mode is predicted. Intermediate values ranging from $n = 0.5$ to 1 suggest the presence of anomalous transport mechanisms.[7] The values of n in this study were as follows: 0.9048 (10% PU), 0.6672 (20% PU), 0.4815 (30% PU), 0.2951 (40% PU), and 0.3188 (50% PU). On

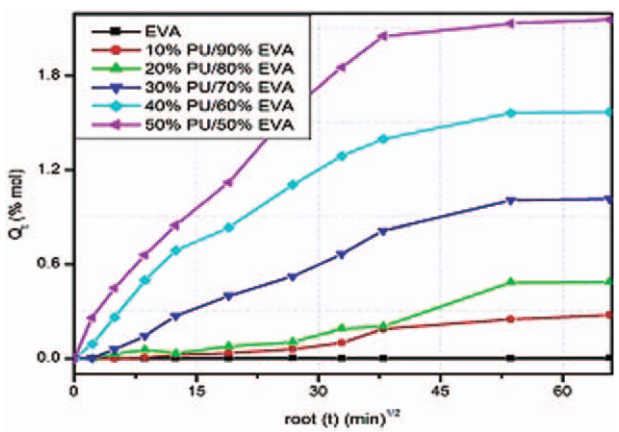

Figure 2 Water sorption versus time profiles. [Color figure can be viewed in the online issue, which is available at wileyonlinelibrary.com.]

TABLE I
Transport Coefficients

Polymer blend	S	D ($\times 10^{-7}$ cm^2/min)	P ($\times 10^{-7}$ cm^2/min)
10% PU/90% EVA	1.050	4.580	4.809
20% PU/80% EVA	1.088	2.334	2.539
30% PU/70% EVA	1.182	8.912	10.53
40% PU/60% EVA	1.282	10.74	13.77
50% PU/50% EVA	1.388	11.48	15.94

the basis of these values, we can state that the transport of water in the polymer blend occurred via Fickian diffusion mode.

Transport coefficients

The moisture diffusion in sheet materials is reported to follow Fick's second law (one-dimensional diffusion).[8] Fick's second law assumes that the absorbed water content (M) is directly proportional to time t, as shown by the following equation:[9]

$$\frac{M-M_i}{M_m-M_i}=1-\frac{8}{\pi^2}\sum_{n=0}^{\infty}\frac{1}{(2n+1)^2}\exp\left[\frac{-D(2n+1)^2\pi^2 t}{h^2}\right] \quad (3)$$

where is D is the diffusion coefficient, which can be calculated by the following equation:[10]

$$D=\pi\left(\frac{h\theta}{4Q_\infty}\right)^2 \quad (4)$$

where θ is the slope of 50% of the initial linear portion of the sorption curves (Q_t vs $t^{1/2}$), Q_∞ is the mass uptake at equilibrium (mol %), and h is the thickness of the polymer blend strip. Another fundamental transport coefficient is the sorption coefficient (S), which is expressed as follows:[10]

$$S=\frac{M_\infty}{M_0} \quad (5)$$

where M_0 is the initial mass of polymer blend and M_∞ is the equilibrium mass.

Another transport coefficient that was considered was the permeation coefficient (P), which was calculated with the following equation:[11]

$$P=DS \quad (6)$$

All of the coefficients are presented in Table I.

The water permeability, D, and S increased with increasing PU content in the polymer blend. The variation in S and P with the PU content was to be expected when we considered that the PU improved the porous nature of the polymer blend. The increase in the transport coefficients underlined the significance of PU in enhancing the water sorption in the hydrophobic EVA polymer.

Pb^{2+} adsorption

The preliminary experiments of this work showed that 3% bentonite/97% EVA could only remove 7.323% of Pb^{2+} from an aqueous solution with an initial concentration of 30 mg/L, whereas 3%bentonite/28.5% PU/68.5% EVA adsorbed 90.00% of Pb^{2+}. On the basis of these results, 3%bentonite/28.5% PU/68.5% EVA was used for all of the adsorption experiments.

Effect of pH

The pH of the solution has a significant impact on the uptake of heavy metals because it determines the surface charge of the adsorbent, degree of ionization, and speciation of the adsorbate.[12–14] The results (Fig. 3) are reported in percentage of Pb^{2+} removal, which was calculated with the following equation:

$$R(\%)=100\times\frac{C_0-C_t}{C_0} \quad (7)$$

where C_0 and C_t are the initial concentration and the concentration at time t, respectively.

A significant increase in the Pb^{2+} removal from aqueous solutions was observed when the pH was increased from 3 to 5. Clay possesses permanent negatively charged sites, which tend to be occupied by H_3O^+ ions, and the remaining positively charged H_3O^+ ions surrounding the adsorbent and the electrostatic density cause electrostatic repulsion between the surface and the Pb^{2+} ions.

The peak at pH 5, which could be assigned to proper Pb^{2+} adsorption as hydroxide ions, came

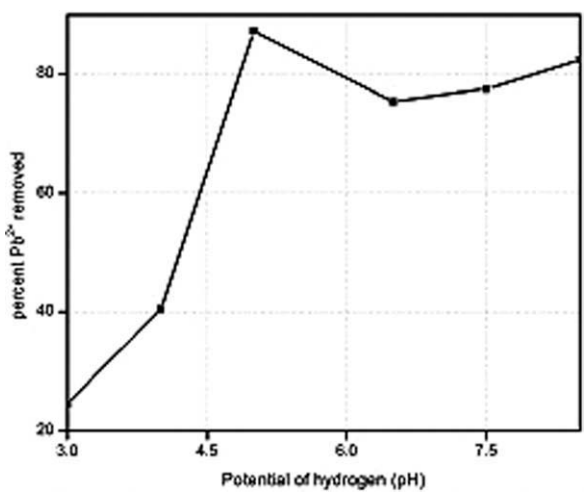

Figure 3 Effect of pH on the adsorption of Pb^{2+} onto the 3% bentonite/28.5% PU/68.5% EVA nanocomposite in 5 h at an initial concentration of 30 mg/L.

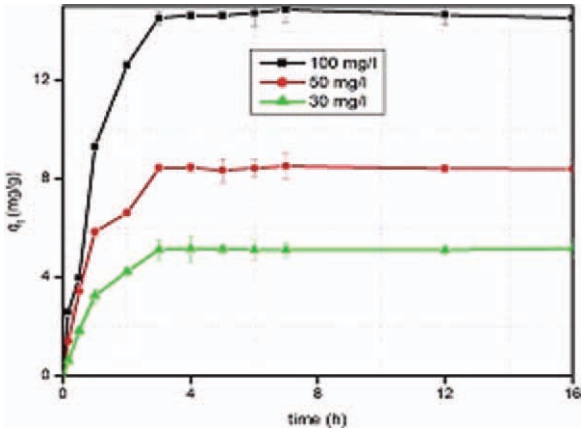

Figure 4 Adsorption time profiles of Pb^{2+} as a function of the initial concentration and contact time. [Color figure can be viewed in the online issue, which is available at wileyonlinelibrary.com.]

closer to balancing the hydronium ions. At pH 6.5, a decrease in the adsorption was observed. This observation could have been due to the coexistence of Pb^{2+}, $Pb(OH)^{+}$, and $Pb(OH)^{2+}$. It is widely accepted that metal species [M(II) = Pb^{2+}] are present in deionized water in the forms of several species, including M^{2+}, $M(OH)^{+}$, $M(OH)_2$, and $M_3(OH)_4^{2+}$,[14] depending on the pH. Beyond pH 7, the results indicate an increasing disappearance of Pb^{2+} with an increase in the solution pH. The increase could be attributed to the hydration of the heavy-metal ions due to the high concentration of hydroxide ions.[12,15] A similar observation was recorded by Hosseini-Bandegharaei et al.[16] on the adsorption of Hg^{2+} on resin containing 1-(2-thiazolylazo)-2-naphthol. At higher pH levels, $M(OH)_2$ is likely to exist in the solid state. Therefore, pH 5 was considered efficient for the retention of Pb^{2+} on the composite and was subsequently used for the rest of the study. Moreover, because the optimum adhesion of Pb^{2+} occurred at pH 5, it can be stated that the removal of Pb^{2+} was mostly through adsorption instead of precipitation. Of course, the possibility of minor nucleation could not be completely ruled out because hydronium ions exist at pH 5. This optimum pH, as well as the results in general, was considered satisfactory on the basis of the Pb speciation diagram presented by Das and Jana.[15]

Adsorption kinetics

The effect of the initial concentration and contact time over the range 0.5–16 h at 20°C was investigated and is reported as the adsorption capacity (q_t). q_t was calculated with the following equation:

$$q_t = \frac{(C_0 - C_t)v}{w_s} \tag{8}$$

where C_0 and C_t represent the initial concentration and the remaining concentration, respectively, at different time intervals, v is the volume of the solution, and w_s is the weight of the composite.

The plots in Figure 4 show the adsorption kinetics of Pb^{2+}. It can be seen that the adsorption of Pb^{2+} on the composite increased steadily until equilibrium was attained after about 3 h. The steep increase in the adsorption capacity during the early stages of the adsorption may have been due to the abundance of adsorption sites available for binding.

In terms of percentage Pb^{2+} removal, the results show that 74% of Pb^{2+} was removed from an initial concentration of 100 mg/L. At an initial concentration of 30 mg/L, the percentage Pb^{2+} removal was found to be 90%. On the basis of these results, it can be stated that the composite can be used for the removal of Pb^{2+} from water. The ability of bentonite to adsorb Pb^{2+} may have been due to the presence of exchangeable ions, aluminol, and silanol groups. The Si—OH and Al—OH have active donor atoms (O) on the surface of the bentonite that are oriented such that their accessibility is not difficult.[13]

Competitive adsorption

The results and discussion in the previous sections have been based only on monosystems of Pb^{2+}. However, under actual real-life circumstances, contaminated water contains several other ions that could have a detrimental effect on the adsorption of heavy metals. Pb/Ag, Pb/Ni, and Pb/Fe binary-component systems were tested to examine the effect of the ionic charge of interfering metals. The uptake of Pb^{2+} in the binary systems was studied at various temperatures, and the results are presented in Figure 5. The percentage Pb^{2+} removed in the binary systems decreased considerably with an increase in the ionic charge of the interfering ion. Furthermore, the adsorption of Pb^{2+} increased with an increase in temperature over the range studied.

The negative effect of interfering ions on the adsorption of Pb^{2+} was also reported by Futalan et al.[17] in a study where chitosan immobilized on bentonite was used as the adsorbent. The variation of the uptake of Pb^{2+} as a function of the competing ions' ionic charge (Z) may be explained by the following equations:

$$M^{+} + Si - OH \rightarrow Si{-}O^{-}M^{+} + H^{+}$$
$$M^{2+} + 2(Si - OH) \rightarrow 2S{-}O^{-}M^{2+} + 2H^{+}$$
$$M^{3+} + 3(Si - OH) \rightarrow 3Si{-}O^{-}M^{3+} + 3H^{+}$$
$$M^{n+} + n(Si - OH) \rightarrow nSi{-}O^{-}M^{n+} + nH^{+}$$

The equations indicate that a metal ion with $Z = n$ (where $n = 1, 2, 3, \ldots \infty$) will occupy n active sites (i.e.,

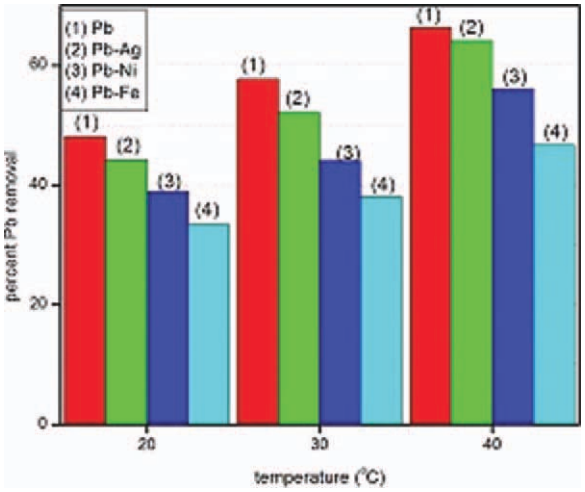

Figure 5 Adsorption of Pb^{2+} in the presence of interfering ions. [Color figure can be viewed in the online issue, which is available at wileyonlinelibrary.com.]

silanol groups). This suggets that one Ag ion may inhabit one active site in the clay and Fe^{3+} may take up three active sites. Basically, the order of Pb^{2+} adsorption inhibition is as follows: $Ag^{+} < Ni^{2+} < Fe^{3+}$.

Thermodynamic studies

The thermodynamic feasibility of the adsorption of Pb^{2+} was studied at 293, 303, and 313 K. The thermodynamic parameters, including Gibbs free energy (ΔG^0), enthalpy (ΔH^0), and entropy (ΔS^0), were determined to obtain a deeper insight into the adsorption of Pb^{2+} by the composite. ΔG^0 was computed with the following equation:

$$\Delta G^0 = -RT \ln K_c \tag{9}$$

where R is the gas constant (8.314 $J \cdot mol^{-1} \cdot K^{-1}$), T is the temperature (K), and K_c is the apparent equilibrium constant of the adsorption and is defined in terms of the Pb^{2+} adsorbed by the composite at equilibrium (C_{ads}) and the equilibrium Pb^{2+} concentration (C_e) and can be calculated by the following equation:[12]

$$K_c = \frac{C_{ads}}{C_e} \tag{10}$$

Values of ΔH^0 and ΔS^0 were obtained from the slope and intercept of the linear plot of ln K_c versus the reciprocal of T:[18]

$$\ln K_c = \frac{\Delta S^0}{R} - \frac{\Delta H^0}{RT} \tag{11}$$

The thermodynamic parameters are summarized and tabulated in Table II. Negative values of ΔG^0 indicate spontaneous adsorption, whereas positive values mean that the adsorption process was nonspontaneous.[14,17,19] Errais et al.[18] reported that negative values of ΔG^0 indicate that the adsorption process is thermodynamically feasible. Therefore, the adsorption of Pb^{2+} was more feasible at 293 K. This means that the observed increase in the adsorption capacity with an increase in temperature could have been due to the enhanced mobility of adsorbate molecules rather than thermodynamic feasibility. The results were consistent with the results presented by Motsa et al.[20] on the adsorption of Pb^{2+} onto polypropylene/clinoptilolite composites, where it was found that the adsorption of Pb^{2+} increased with an increase in temperature up to 313 K. Moreover, Sölener et al.[21] stated that ΔG^0 for physical adsorption ranges between magnitudes of 20 and 0 kJ/mol and generally ranges between 20 and 80 kJ/mol in cases of the coexistence of chemisorption and physisorption. The ΔG^0 values shown in Table II demonstrate that the removal of Pb^{2+} was mostly through physical adsorption.

The negative values of ΔH^0 suggested that the adsorption process was exothermic.[13] Moreover, like ΔG^0, the magnitude of ΔH^0 could be used to predict the dominant mechanism involved in the adsorption process, that is, chemical or physical interactions. Adsorption enthalpies over the range 80–420 kJ/mol signify electrostatic adsorption. Rahmani et al.[12] reported that an enthalpy of less than 80 kJ/mol indicates that the adsorption involves physisorption. According to Li et al.,[22] a physical adsorption enthalpy in the range 4–8 kJ/mol indicates van der Waals interactions, whereas one in the range 8–40 kJ/mol indicates hydrogen bonding as the main interaction. As can be seen from Table II, the removal of Pb^{2+} in this study was mostly through hydrogen bonding between the bentonite and the adsorbate; this suggested that the adsorbed metal was hydrated. The negative ΔS^0 values signified that there was a decrease in the randomness at the nanocomposite/Pb^{2+} solution interface,[13,18] probably due to the nonuniform surface morphology of the composite, as exhibited by the SEM pictures.

Adsorption isotherms

The equilibrium results are reported in terms of the amount of Pb^{2+} adsorbed at equilibrium per unit weight of the composite [q_e (mg/g)], which can be represented as follows:

$$q_e = \frac{(C_o - C_e)v}{w_s} \tag{12}$$

TABLE II
Adsorption Thermodynamic Parameters

T (K)	ΔG^0 (kJ/mol)	ΔH^0 (kJ/mol)	ΔS^0 ($J \cdot mol^{-1} \cdot K^{-1}$)
293	−2.140		
303	8.489	−28.56	−96.83
313	17.89		

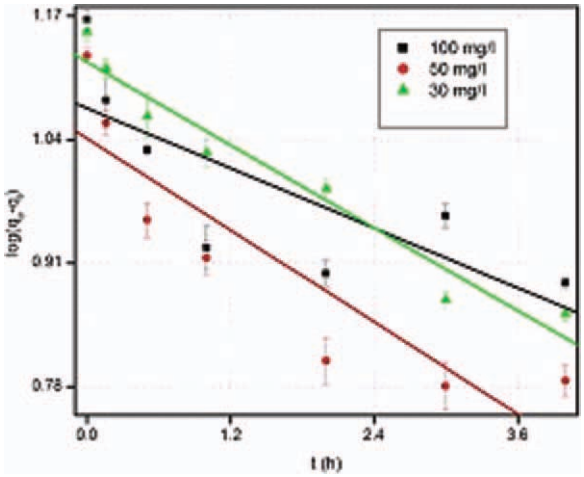

Figure 6 Pseudo-first-order model. [Color figure can be viewed in the online issue, which is available at wileyonlinelibrary.com.]

The Langmuir and Freundlich models are widely applied in adsorption isotherms.[23] The Langmuir isotherm assumes monolayer adsorption and is expressed as follows:

$$\frac{C_e}{q_e} = \frac{1}{bQ_0} + \frac{C_e}{Q_0} \tag{13}$$

where Q_0 is the adsorption capacity (mg/g) and b is the energy of adsorption (ℓ/mg).[24]

If the data fit a Langmuir isotherm, a plot of C_e/q_e versus C_e should give a linear plot (results not shown here). The correlation coefficient was found to be 0.9869.

The essential feature of the Langmuir isotherm is the equilibrium parameter (R_L), a dimensionless constant that can be presented as follows:

$$R_L = \frac{1}{1 + bC_0} \tag{14}$$

The value of R_L was found to be 0.0905. R_L indicates whether the adsorption is unfavorable ($R_L > 1$), linear ($R_L = 1$), favorable ($0 < R_L < 1$), or irreversible ($R_L = 0$).[21,25] Therefore, the adsorption of Pb^{2+} onto the composites was favorable under conditions used in this study.

The Freundlich model is employed to describe heterogeneous systems. The isotherm assumes that the adsorbent surface sites have an array of different binding energies:[25]

$$\log q_e = \log K_F + \frac{1}{n}\log C_e \tag{15}$$

where C_e is the equilibrium concentration of the adsorbate and K_F and n are the Freundlich constants, which can be determined from the linear graph of log q_e against log C_e. The results are not shown here. The model had a correlation coefficient of 0.9599.

The primary constant in the Freundlich model is n, which is a measure of the deviation from linearity of the adsorption. Bello et al.[26] stated that if $n < 1$ then the process is governed by chemical adsorption. The value of n was found to be 2.449, and it implied that the adsorption of Pb^{2+} onto the composite was favorable and governed mostly by physical adsorption rather than chemical adsorption. On the basis of the correlation coefficients, the adsorption process may have best been defined with the Langmuir adsorption isotherm. The results suggests a monolayer formation onto the homogeneous composite surface; hence, each Pb^{2+} ion was located on a single-adsorption site. On a homogeneous surface, adsorption occurs at constant energies, and all of the adsorption surface sites have identical adsorbate affinities, whereas on a heterogeneous surface, adsorption occurs at energies that are distributed over the surface.[19,27]

Kinetic models

To check the applicability of the rate law, the kinetic data were fitted to the pseudo-first-order equation and pseudo-second-order equation. The pseudo-first-order equation is expressed as follows:

$$\log(q_e - q_t) = \log q_e - \frac{k_1}{2.303}t \tag{16}$$

where q_t refers to the amount of Pb^{2+} (mg/L) adsorbed on the composite at time t (h) and k_1 is the Lagergren rate constant (h^{-1}). Plotting log($q_e - q_t$) versus t should yield a linear graph where the experimental equilibrium adsorption capacity [$q_{e,exp}$] is extrapolated from the y intercept. The results are shown in Figure 6, and the tabulated constants are summarized and shown in Table III. The correlation coefficients were found to be 0.6029 (100 mg/L), 0.7990 (50 mg/L), and 0.9506 (30 mg/L).

The pseudo-second-order reaction kinetic model is expressed as follows:[23]

$$\frac{t}{q_t} = \frac{1}{k_2 q_e^2} + \frac{t}{q_e} \tag{17}$$

TABLE III
Adsorption Capacity Tabulated from the Kinetic Models and Δq Values

C_0 (mg/L)	Mean $q_{e,exp}$	Pseudo-first-order		Pseudo-second-order	
		$q_{e,cal}$	Δq (%)	$q_{e,cal}$	Δq (%)
100	14.86	10.44	8.847	15.41	0.1370
50	8.504	9.020	0.3682	8.787	0.1107
30	5.158	10.69	115.0	5.461	0.3451

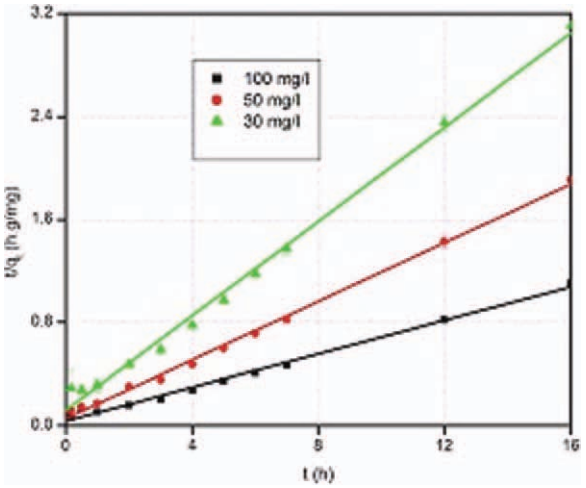

Figure 7 Pseudo-second-order model. [Color figure can be viewed in the online issue, which is available at wileyonlinelibrary.com.]

where k_2 is the second-order rate constant. If second-order kinetics are applicable, t/q_t should show a linear relationship with t, as shown in Figure 7, and the extrapolated constants, as given in Table III. The correlation coefficients were found to be 0.9938 (100 mg/L), 0.9971 (50 mg/L), and 0.9943 (30 mg/L).

The pseudo-second-order equation gave higher correlation coefficient values compared to the pseudo-first-order equation at identical initial concentrations; this showed that the retention of Pb^{2+} from aqueous solution adhered to the pseudo-second-order rate law.[28] This observation suggests that the extraction of Pb^{2+} from the aqueous media occurred through monolayer adsorption, as established by the adsorption isotherms.

Validation of kinetic models

The best fit among the kinetic models was further assessed quantitatively by the normalized standard deviation [Δq (%)], which can be expressed as follows:

$$\Delta q(\%) = 100\sqrt{\frac{\sum\left[\left(q_{e,\exp} - q_{e,\mathrm{cal}}\right)/q_{e,\exp}\right]^2}{N-1}} \qquad (18)$$

where $q_{e,\mathrm{cal}}$ is the calculated saturation adsorption amount and $N - 1$ is the degrees of freedom. The Δq (%) values are given in Table III.

There was a good degree of agreement between $q_{e,\exp}$ and $q_{e,\mathrm{cal}}$ from the pseudo-second-order model, as can be seen from Table III. The values implied that, indeed, the adsorption of Pb^{2+} onto the nanocomposite may have best been described through pseudo-second-order kinetics.

CONCLUSIONS

In this study, we demonstrated that the EVA/PU polymer blend has the potential to be applied in water environments, especially in the field of heavy-metal removal technologies. It was established that the polymer blend formed a suitable matrix in polymer/clay composites. The bentonite/PU/EVA composite was tested for the extraction of Pb^{2+} from water, and it was found that equilibration was attained in 3 h, despite the hydrophobic nature of EVA, which was the major constituent.

The authors thank G&W Minerals for supplying the bentonite clay.

References

1. Dinesh, M.; Kunwar, P. S. Water Res 2002, 36, 2304.
2. Nadeem, G.; Mahmood, A.; Shahid, S. A.; Shah, S. S.; Khalid, A. M.; McKay, G. J Hazard Mater B 2006, 138, 604.
3. Vargas, A. M. M.; Cazetta, A. L.; Garcia, C. A.; Moraes, J. C. G.; Nogami, E. M.; Lenzi, E.; Costa, W. F.; Almeida, V. C. J Environ Manage 2011, 92, 178.
4. Tongpoothorn, W.; Sriuttha, M.; Homchan, P.; Chanthai, S.; Ruangviriyachai, C. Chem Eng Res Des 2011, 89, 335.
5. Lai, M.; Chang, K.; Yeh, J.; Liou, S.; Hsieh, M.; Chang, H. Eur Polym J 2007, 43, 4219.
6. Bessadok, A.; Marais, S.; Gouanvé, F.; Colasse, L.; Zimmerlin, I.; Roudesli, S.; Métayer, M. Compos Sci Technol 2007, 67, 685.
7. Dlamini, D. S.; Mishra, S. B.; Mishra, A. K.; Mamba, B. B. J Inorg Orgonomet Polym 2011, 21, 229.
8. Ladhari, A.; Daly, H. B.; Belhadjsalah, H.; Cole, K. C.; Denault, J. Polym Degrad Stab 2010, 95, 1.
9. Jost, W. Diffusion in Solids, Liquids, Gases; Academic: New York, 1960.
10. Satheesh, M. N.; Kumar, K. S.; Siddaramaiah, M. J Hazard Mat 2007, 145, 36.
11. Mathew, A. P.; Packirisamy, S.; Kumaran, M. G.; Thomas, S. Polymer 1995, 36, 4935.
12. Rahmani, A.; Mousavi, H. Z.; Fazli. M. Desalination 2010, 253, 94.
13. Wang, Q.; Chan, X.; Li, D.; Hu, Z.; Li, R.; He, Q. J Hazard Mater 2011, 186, 1076.
14. Sen, T. K.; Gomez, D. Desalination 2011, 267, 286.
15. Das, N.; Jana, R. K. J Colloid Interface Sci 2006, 293, 253.
16. Hosseini-Bandegharaei, A.; Hosseini, M. S.; Jalalabadi, Y.; Sarwghadi, M.; Nedaie, M.; Aherian, A.; Ghaznavi, A.; Eftekhari, A. Chem Eng J 2010, 168, 1163.
17. Futalan, C. M.; Kan, C.-C.; Dalida, M. L.; Hsien, K.-J.; Pascua, C.; Wan, M.-W. Carbohydr Polym 2011, 83, 528.
18. Errais, E.; Duplay, J.; Darragi, F.; M'Rabet, I.; Aubert, A.; Huber, F.; Morvan, G. Desalination 2011, 275, 74.
19. Keun-Young, S.; Jin-Yong, H.; Jyongsik, J. J Hazard Mater 2010, 190, 36.
20. Motsa, M. M.; Mamba, B. B.; Thwala, J. M.; Msagati, T. A. M. J Colloid Interface Sci 2011, 359, 210.
21. Sölener, M.; Tunali, S.; Özcan, A. S.; Gedikbey, A. T. Desalination 2008, 223, 308.
22. Li, X.; Zhou, Q.; Wei, S.; Ren, W.; Sun, X. Geoderma 2011, 160, 347.
23. Doulia, D.; Leodopoulos, C.; Gimouhopoulos, K.; Rigas, F. J Colloid Interface Sci 2009, 340, 131.
24. Abdel-Halim, S. H.; Shehata, A. M. A.; El-Shahat, M. F. Water Res 2003, 37, 1678.
25. Olu-Owolabi, B. I.; Unuabonah, E. I. Appl Clay Sci 2011, 51, 170.
26. Bello, O. S.; Adelaide, O. M.; Abdul, H. M.; Abdul, M. P. O. Macedonian J Chem Chem Eng 2010, 29, 77.
27. Marsalek, R.; Pospisil, J.; Taraba, B. Colloids Surf A 2011, 383, 80.
28. Zhi-Rong, L.; Shao-Qi, Z. Process Saf Environ Prot 2010, 88, 62.